Electronic Supplementary Material (ESI) for Journal of Materials Chemistry C.

Multifunctional Application of Triazine/Carbazole Hybrid Thermally Activated Delayed Fluorescence Emitters in Organic Light Emitting Diodes

Di Liu,[a]* Deli Li,[a] Huihui Meng,[a] Ying Wang,[b]* Lizhu Wu[b]*

[a] State Key Laboratory of Fine Chemicals, College of Chemistry, Dalian University of Technology, 2 Linggong Road, Dalian, 116024, China. E-mail: liudi@dlut.edu.cn

[b] Key Laboratory of Photochemical Conversion and Optoelectronic Materials, Technical Institute of Physics and Chemistry, The Chinese Academy of Sciences, Beijing 100190, China. E-mail: E-mail: wangy@mail.ipc.ac.cn, lzwu@mail.ipc.ac.cn

Contents

1. Experimental Section

General information. The ^{1}H NMR and ^{13}C NMR spectra were recorded using a 400 MHz and 126 MHz Bruker Avance II 400 and Bruker AVANCE Ⅲ 500. The mass spectra were recorded on a HP1100LC/MSD MS spectrometer. The fluorescence and UV-vis absorption spectra measurements were performed on a Perkin-Elmer LS55 spectrometer and a Perkin-Elmer Lambda 35 spectrophotometer, respectively. The phosphorescence spectra were measured in 2-MeTHF glass matrix at 77 K using a Hitachi F-4600 fluorescence spectrometer. Temperature dependent transient PL spectra were measured with an Edinburgh FLS920 fluorescence spectrophotometer. Temperature transient PL decay was measured with an Edinburgh FLS920 fluorescence spectrophotometer. Thermogravimetric analyses (TGA) was performed on a Perkin-Elmer thermogravimeter (Model TGA7) under a N_2 flow at a heating rate of 10 ℃ min^{-1}. DSC measurements were operated on a Netzsch DSC 201 under a N_2 flow at a heating rate of 10 ℃ min^{-1} and cooling by liquid nitrogen. Cyclic voltammogram (CV) were carried out using a conventional three electrode configuration and an electrochemical workstation (BAS100B, USA) at a scan rate of 100 mV s^{-1}. A glass carbon working electrode, a Pt-wire counter electrode, and a saturated calomel electrode (SCE) reference electrode were used. All of the measurements were made at room temperature on deoxygenated samples in dichloromethane with 0.1 M $[Bu_4N]PF_6$ as the electrolyte.

OLED fabrication and measurements. The pre-cleaned ITO glass substrates, with a sheet resistance of 15 Ω m^{-2}, were treated by UV-ozone for 30 min. A 40 nm

thick PEDOT: PSS film was spin coated on the ITO glass substrate firstly and baked at 120 ℃ for 30 min in air. Subsequently, the substrate was transferred into a vacuum chamber to deposit the organic layers with a base pressure of less than 10^{-6} Torr (1 Torr =133.32 Pa). A 1 nm thin layer of LiF and a subsequently 200 nm thin layer of Al were vacuum deposited as the cathode. Deposition rates are 0.1 Å s^{-1} for LiF and 6 Å s^{-1} for Al. The emitting area of each pixel was determined by the overlapping of the two electrodes and was 9 mm^2. The EL spectra, CIE coordinates and *J–V–B* curves of the devices were measured with a PR705 photometer and a source-measure-unit Keithley 236 under ambient conditions at room temperature. The forward viewing external quantum efficiency was calculated by using the current efficiency, EL spectra and human photopic sensitivity.

Quantum Chemical Computation. All of the simulations were performed using the Gaussian 09_D01 program package.[1] Detailed calculation approach affording $E_{0\text{-}0}$ (^{1}CT), $E_{0\text{-}0}$ (^{3}CT) and $E_{0\text{-}0}$ (^{3}LE) are shown in Equation S1 to S3.[2] More details of analysis data are shown in Table S1. The analysis of CT amount (q) of the investigated compounds was conducted using Multiwfn program.[3] Then the optimized Hartree-Fock percentage was confirmed by OHF%=42q relationship. The confirmation of E_{VA} (S_1, OHF) was fitted from a straight line between the E_{VA} (S_1) values yielded by two functions with the closest HF% to the OHF%. In relationship S3, the correction factor C is found to be 1.10, 1.18 and 1.30 for BMK, M06-2X and M06-HF, respectively.

$$E_{0-0}(^1CT) = E_{VA}(S_1, OHF) - 0.24 \quad \text{(S1)}$$

$$E_{0-0}(^3CT) = E_{0-0}(S_1) - [E_{VA}(S_1, OHF) - \frac{E_{VA}(S_1, OHF)}{E_{VA}(S_1, BLYP)} E_{VA}(T_1, BLYP)] \quad \text{(S2)}$$

$$E_{0-0}(^3LE) = E_{VA}(T_1) / [E_{VA}(S_1, OHF) / E_{VA}(S_1, BLYP)] - 0.09 \quad \text{(S3)}$$

Materials. All solvents and reagents were used as received from commercial suppliers without any further purification. The hole transporting materials (TAPC) and electron transporting materials (TmPyPB) were purchased from Lumtec Co., Ltd. The host materials (mCP) were purchased from Xi'an Polymer Light Technology Corp..

Compound Synthesis and Characterization.

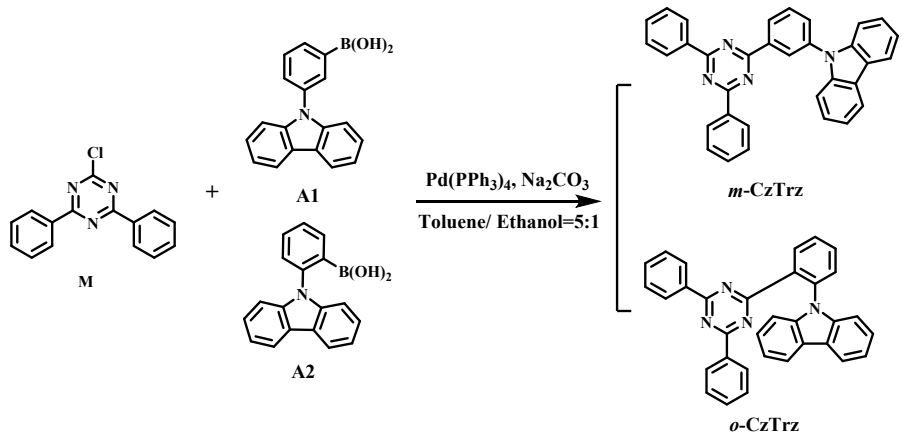

9-(2-(4,6-Diphenyl-1,3,5-triazin-2-yl)phenyl)-9*H*-carbazole (*o*-CzTrz) was synthesized according to the literature method.[4]

Synthesis of 9-(3-(4,6-diphenyl-1,3,5-triazin-2-yl)phenyl)-9H-carbazole (m-CzTrz):[5] To a mixed solution of intermediate M (200 mg, 0.75 mmol), the boronic acid A2 (240 mg, 0.8 mmol), toluene (20 mL), ethanol (4 mL) and aqueous sodium carbonate (2 M, 7.5 mL, 14.9 mmol), tetrakis(triphenylphosphino)palladium(0) (17.3 mg, 0.02 mmol) was added under nitrogen atmosphere. The reaction mixture was refluxed overnight. Upon cooling to room temperature and diluting with water (20

mL), the organic layer was separated and the aqueous layer was extracted with dichloromethane (3 × 20 mL). The combined organic layers were washed with brine (50 mL), dried over anhydrous magnesium sulfate and filtered. After removing the solvent under reduced pressure, the residue was purified by column chromatography over silica using petroleum ether/dichloromethane as eluent, followed by repeated recrystallization in methanol/chloroform to give pure final product. Light green solid. Yield: 64.9%. ^{1}H NMR (400 MHz, $CDCl_3$) δ: 8.98 (s, 1H), 8.92-8.85 (m, 1H), 8.80-8.72 (m, 4H), 8.20 (d, *J*=7.8 Hz, 2H), 7.88-7.75 (m, 2H), 7.65-7.52 (m, 6H), 7.46 (ddd, *J* = 10.5, 9.2, 4.4 Hz 4H), 7.37-7.29 (m, 2H). ^{13}C NMR (126 MHz, $CDCl_3$) δ: 171.86, 170.93, 140.96, 138.46, 138.26, 135.95, 132.68, 131.15, 130.24, 129.02, 128.68, 128.03, 127.68, 126.12, 123.45, 120.38, 120.09, 109.78. TOF-EI-MS (*m/z*): 474.1841 (M^+). Anal. calcd for $C_{33}H_{22}N_4$: C, 83.52; H, 4.67; N, 11.81. Found: C, 83.43; H, 4.65; N, 11.92.

2. Supplemental Tables and Figures

Table S1. The fitted parameters of *o*-CzTrz and *m*-CzTrz.

compounds	CT amount (q)	OHF (%)	E_{VA} (S_1,OHF) (eV)	$E_{0\text{-}0}$ (^{1}CT) (eV)	$E_{0\text{-}0}$ (^{3}CT) (eV)	$E_{0\text{-}0}$ (^{3}LE) (eV)	ΔE_{ST} (eV)
o-CzTrz	0.866	36.4	3.20	2.96	2.94	2.90	0.06
m-CzTrz	0.863	36.2	3.33	3.09	2.99	2.86	0.23

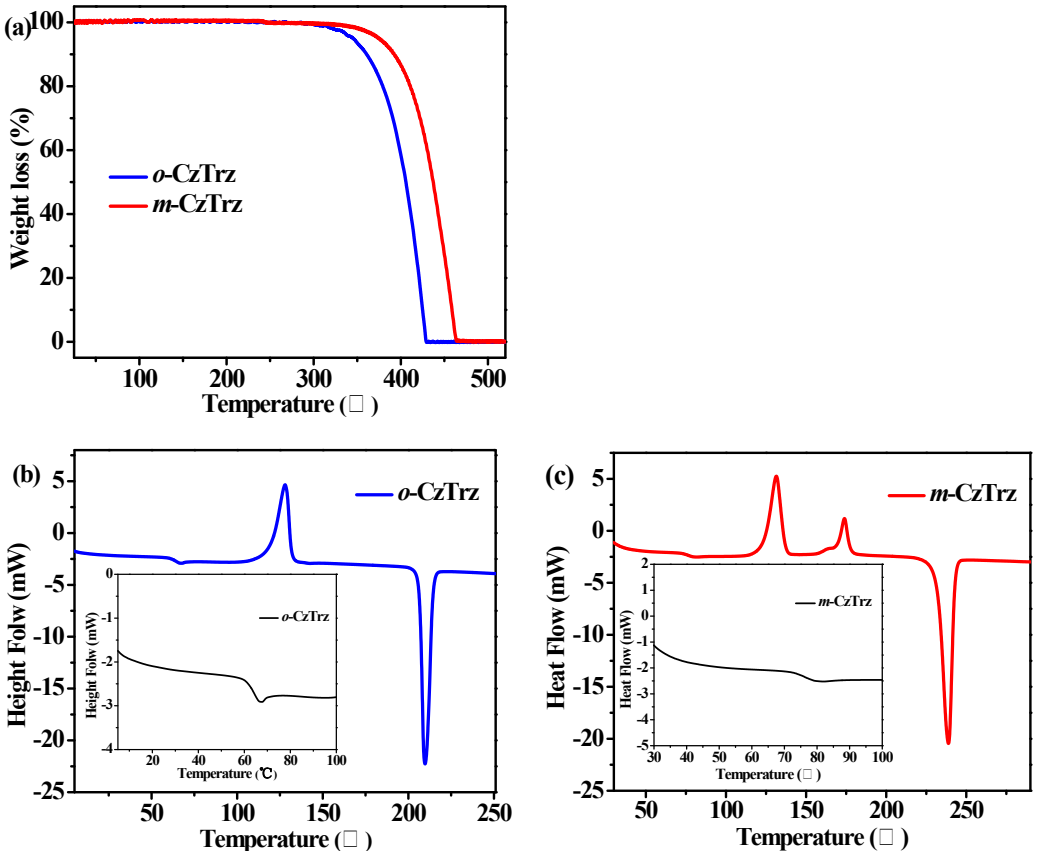

Fig. S1 TGA (a) and DSC (b and c) curves of *o*-CzTrz and *m*-CzTrz.

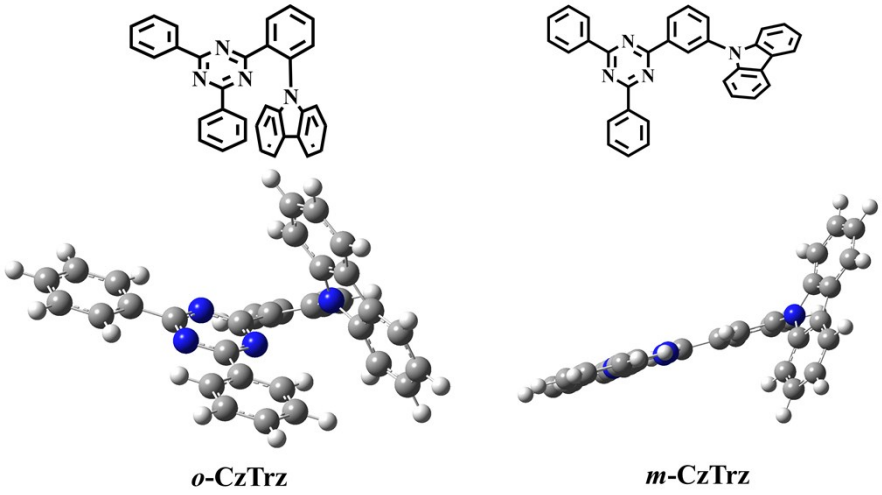

Fig. S2 Steric conformations of *o*-CzTrz and *m*-CzTrz in ground state. Both carbazole and triazine rings are almost perpendicular to the phenylene bridge plane with dihedral angles of 64.5° and 35°, generating an approximate face-to-face arrangement of donor and acceptor rings. While the triazine ring is on the same plane with the phenylene bridge in *m*-CzTrz, and the carbazole ring has a dihedral angle of 53.6° with the bridge plane.

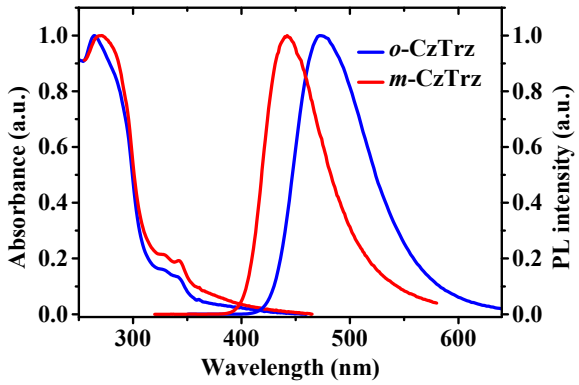

Fig. S3 UV-vis absorption and PL spectra of *o*-CzTrz and *m*-CzTrz in solid thin films at 300 K.

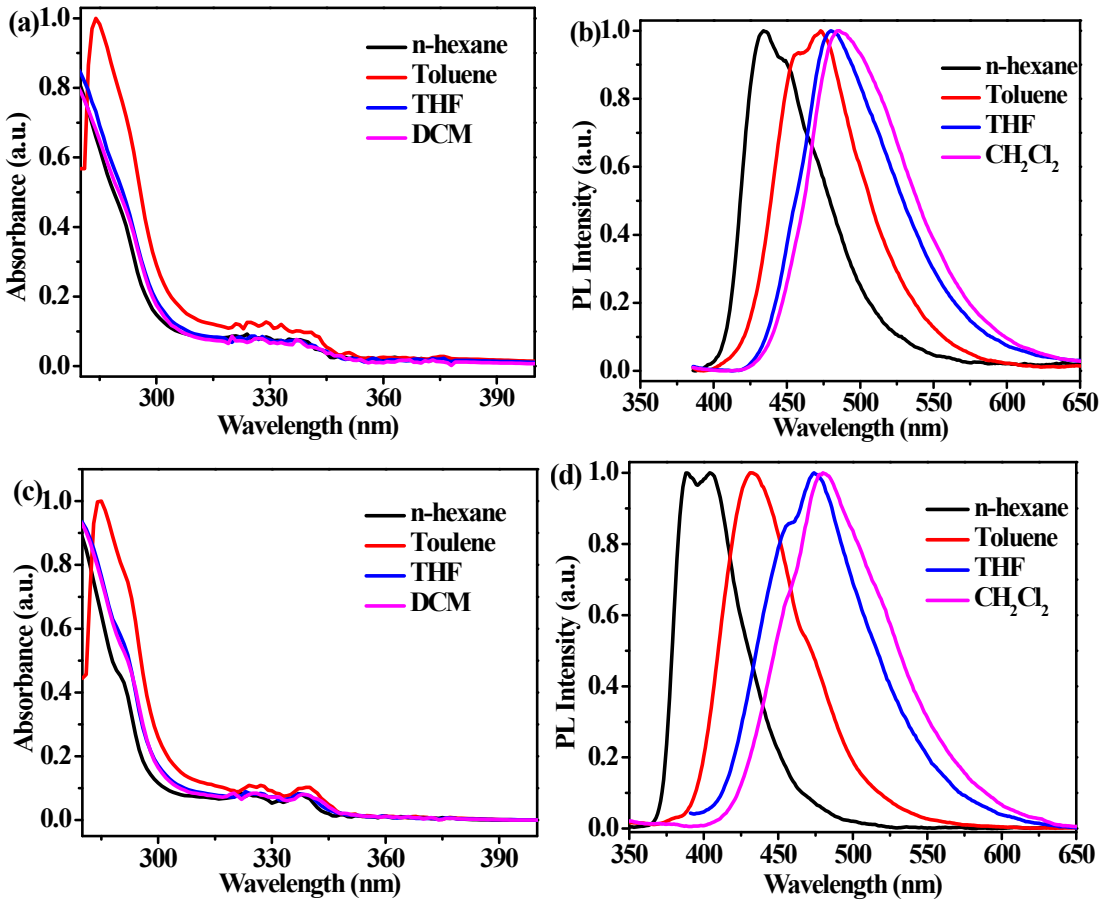

Fig. S4 UV-vis absorption and PL spectra of *o*-CzTrz (a, b) and *m*-CzTrz (c, d) in different polar solvents at 300 K.

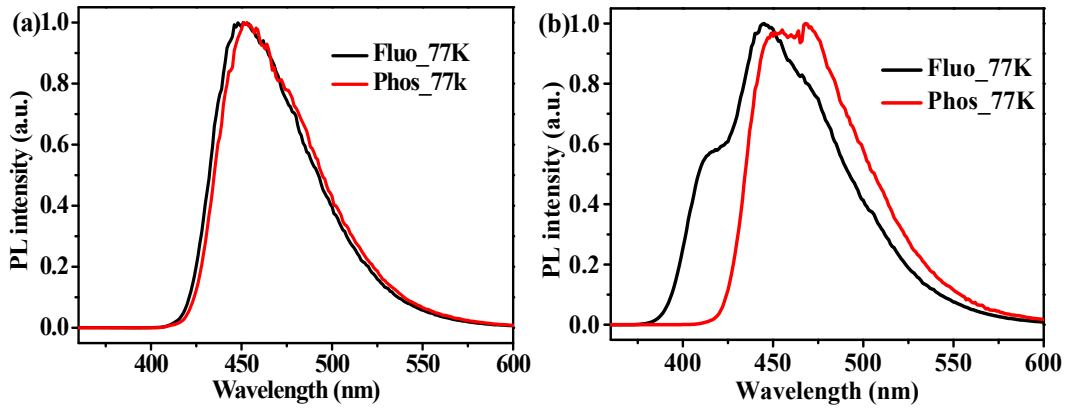

Fig. S5 Fluorescence and phosphorescent spectra of *o*-CzTrz (a) and *m*-CzTrz (b) in frozen 2-MeTHF at 77 K.

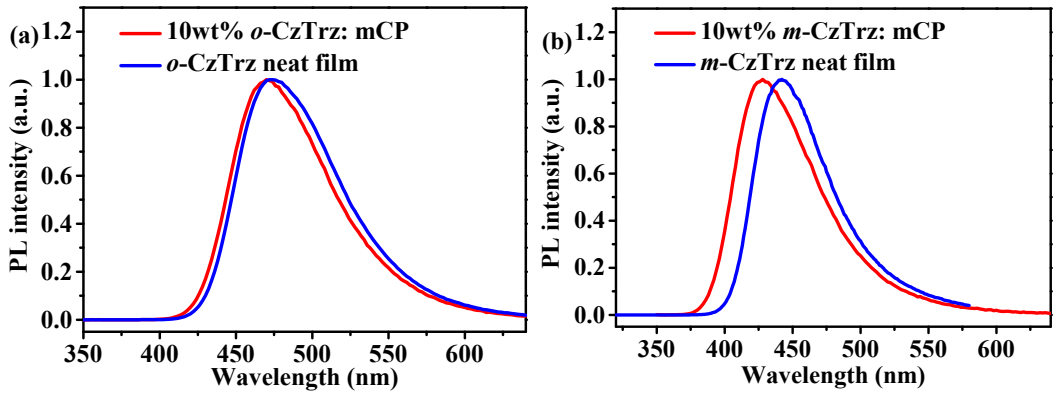

Fig. S6 PL spectra of *o*-CzTrz (a) and *m*-CzTrz (b) doped and neat films.

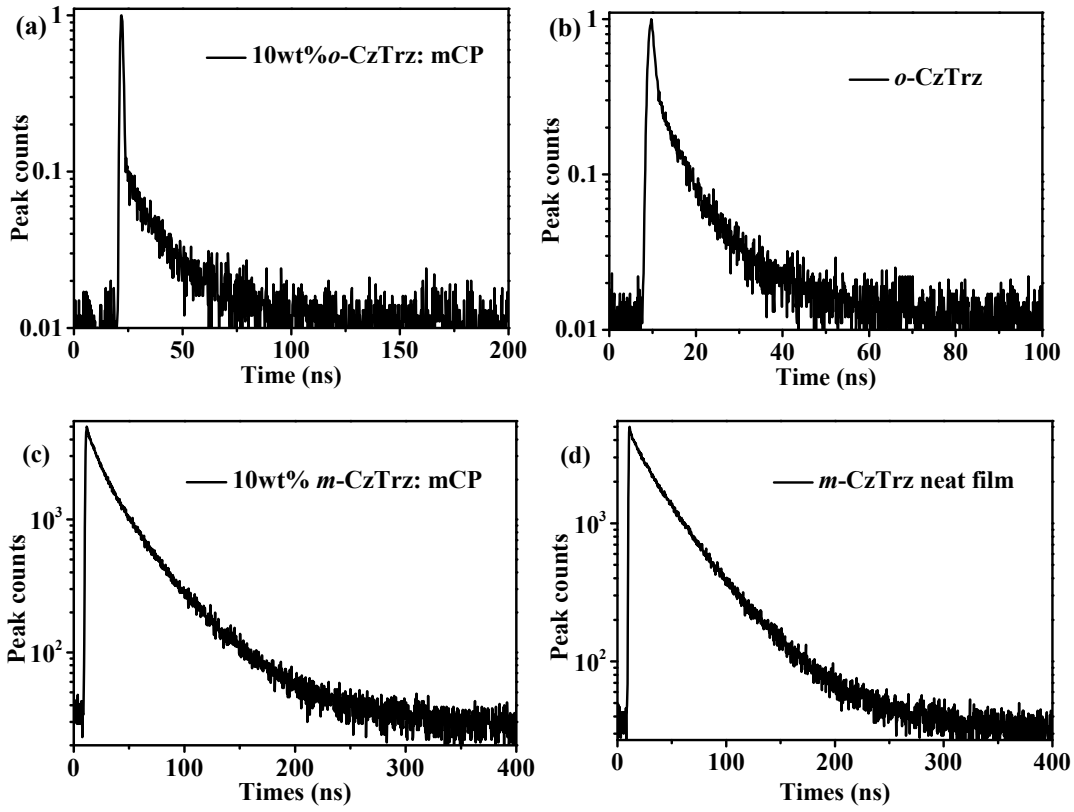

Fig. S7 Transient PL decay of the solid thin film. (a) 10wt% *o*-CzTrz: mCP film. (b) *o*-CzTrz neat film. (c) 10wt% *m*-CzTrz: mCP film. (d) *m*-CzTrz neat film.

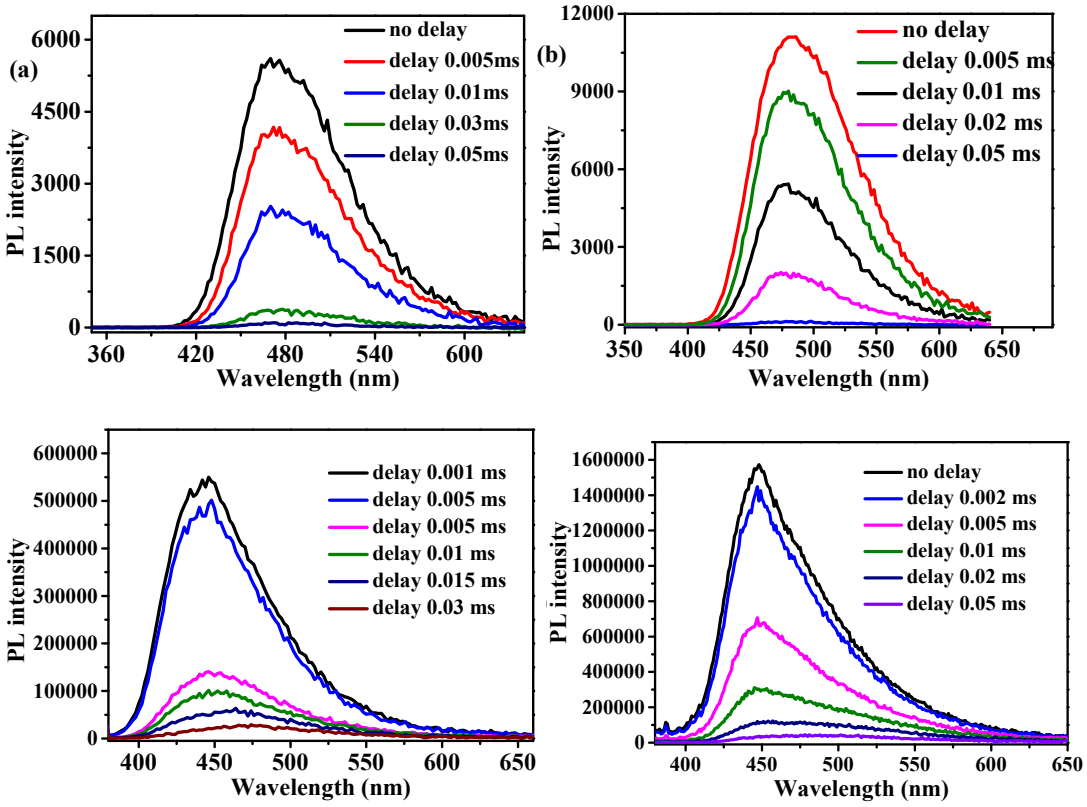

Fig. S8. Delayed fluorescence spectra of *o*-CzTrz and *m*-CzTrz in doped and neat films at 300 K. (a) 10 wt% *o*-CzTrz: mCP film. (b) *o*-CzTrz neat film. (c) 10 wt% *m*-CzTrz: mCP film. (d) *m*-CzTrz neat film.

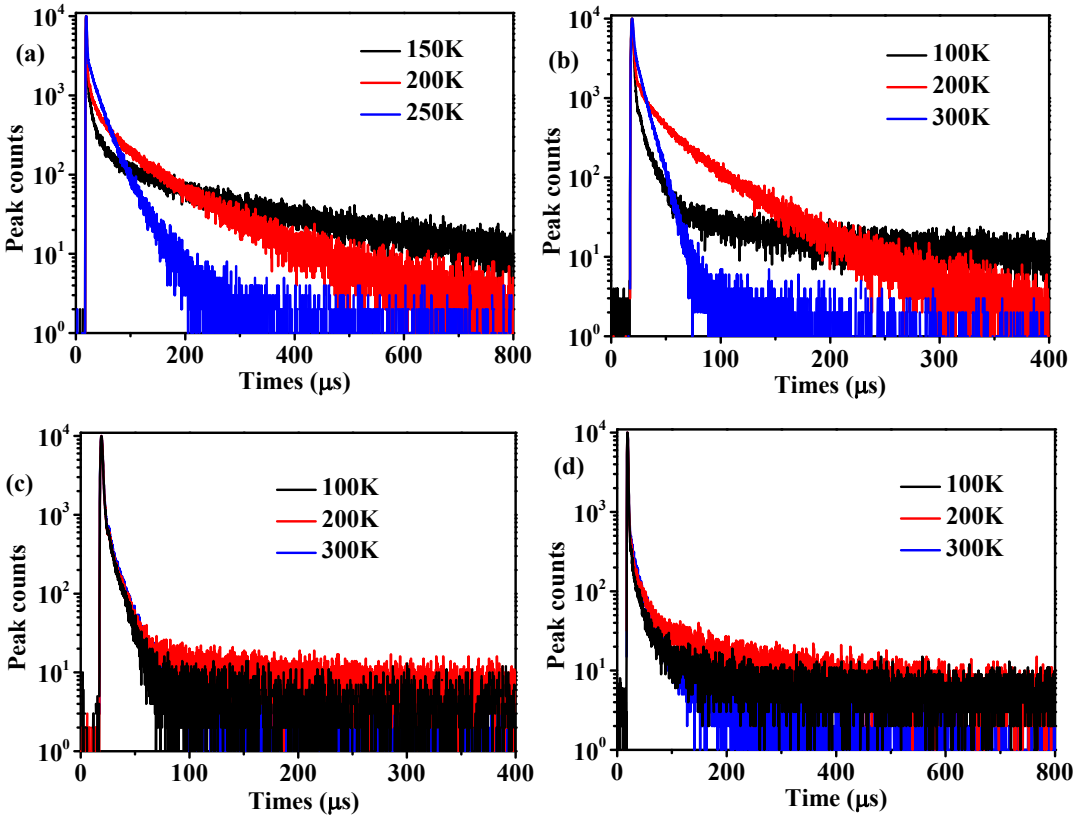

Fig. S9 Transient PL decay of the solid thin film at different temperature. (a) 10 wt% *o*-CzTrz:mCP film. (b) *o*-CzTrz neat film. (c) 10 wt% *m*-CzTrz:mCP film. (d) *m*-CzTrz neat film.

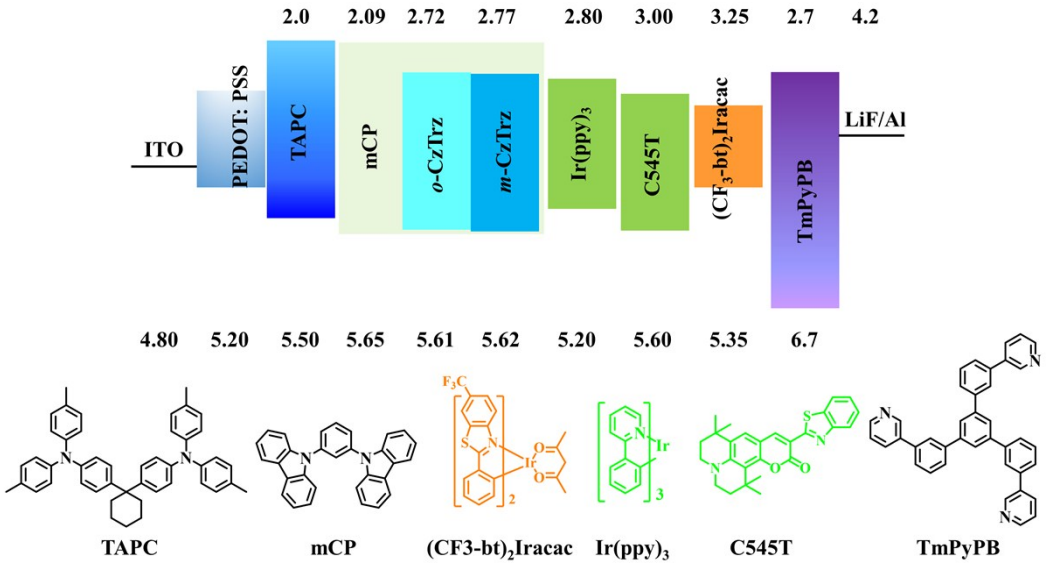

Fig. S10 Chemical structures of related materials and energy level diagram for the TADF OLEDs and hybrid WOLEDs.

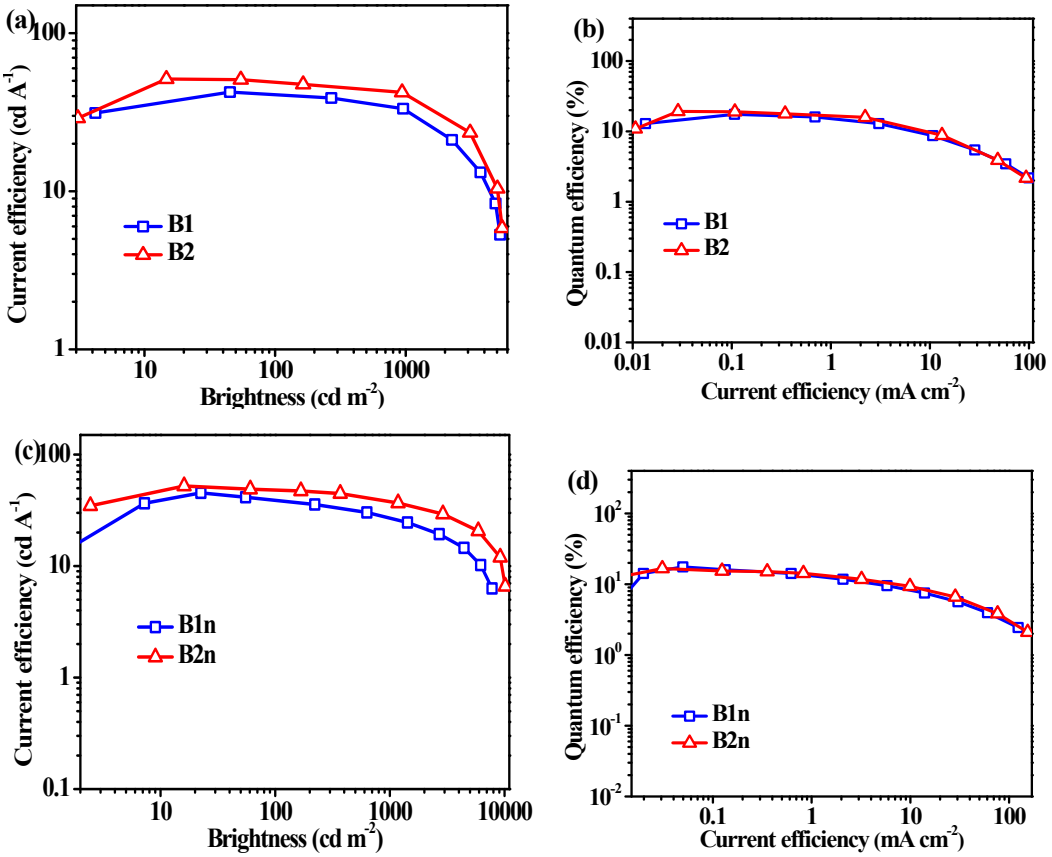

Fig. S11 Efficiency curves (a, b, c, d) of the greenish-blue doped OLEDs B1 and B2 and non-doped devices B1n and B2n.

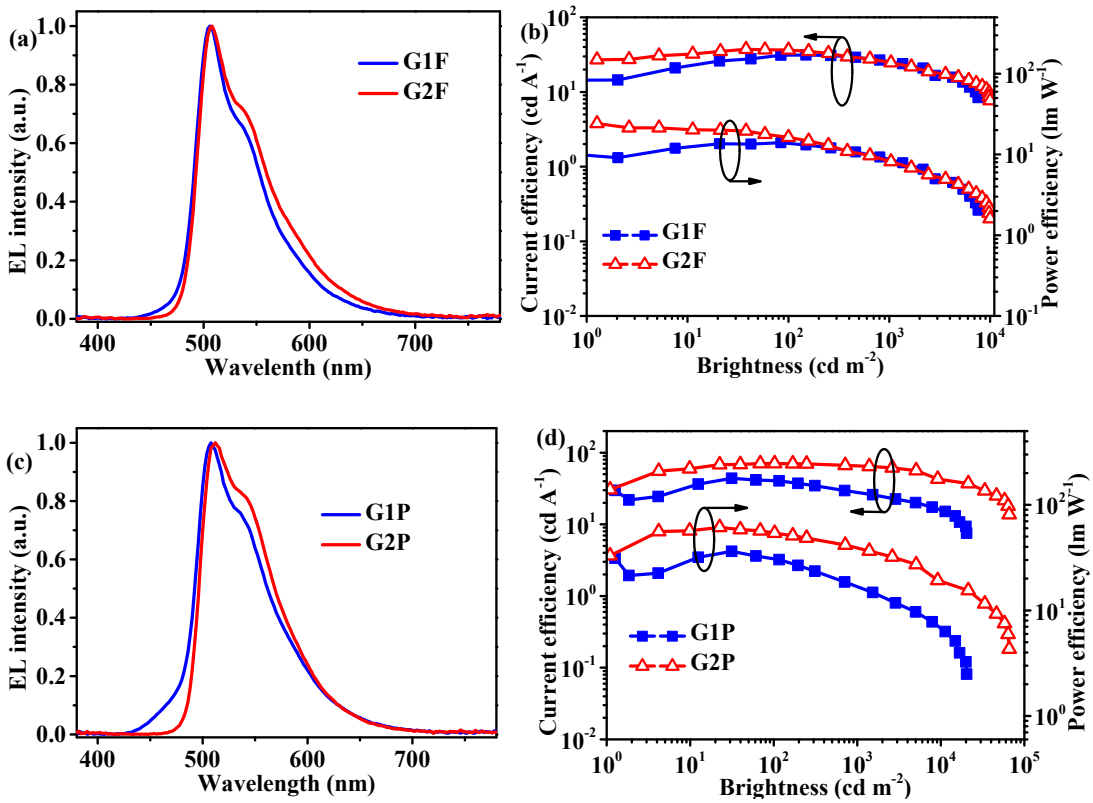

Fig. S12 EL spectra and efficiency curves of *o*-CzTrz and *m*-CzTrz hosted green fluorophors (a, b) and phosphors (c, d).

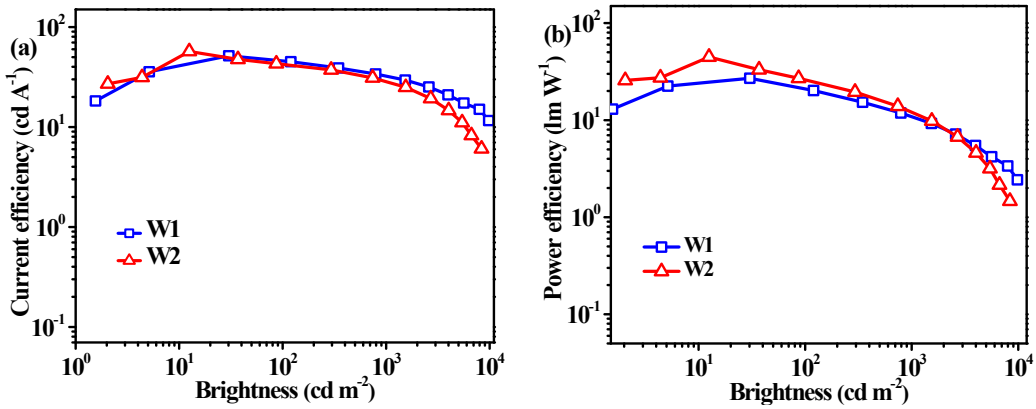

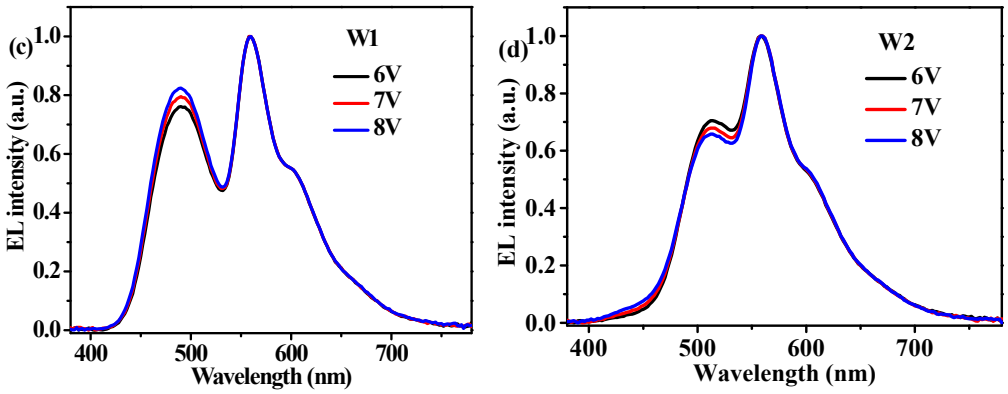

Fig. S13 Efficiency curves (a, b) and voltage-dependent EL spectra (c, d) for hybrid white OLEDs.

3. References

1 M. J. Frisch, G. W. Trucks, H. B. Schlegel, et al. *Gaussian 09*, Revision D_01. Gaussian, Inc.: Wallingford CT, 2009.

2 S. Huang, Q. Zhang, Y. Shiota, T. Nakagawa, K. Kuwabara, K. Yoshizawa, and C. Adachi, *J. Chem. Theory Comput.,* 2013, **9**, 3872.

3 T. Lu, F. Chen, *J. Comput. Chem.*, 2012, **33**, 580.

4 J.-R. Cha, C. W. Lee, J. Y. Lee, M.-S. Gong, *Dyes Pigm.*, 2016, **134**, 562.

5 (a) W. Li, J. Li, D. Liu, D. Li, D. Zhang, *Chem. Sci.*, 2016, **7**, 6706. (b) L. Deng, J. Li, G.-X. Wang, L-Z. Wu, *J. Mater. Chem. C*, 2013, **1**, 8140.